

Article

Neuroprotective Effects of Fingolimod in a Cellular Model of Optic Neuritis

Amritha A. Candadai ^{1,2,3}, Fang Liu ^{1,2,3} , Arti Verma ^{1,2}, Mir S. Adil ^{1,2} , Moaddey Alfarhan ^{1,2,3}, Susan C. Fagan ^{1,2}, Payaningal R. Somanath ^{1,2}  and S. Priya Narayanan ^{1,2,3,*}

- ¹ Clinical and Experimental Therapeutics Program, College of Pharmacy, University of Georgia, Augusta, GA 30912, USA; amritha@uga.edu (A.A.C.); fliu1@augusta.edu (F.L.); Av01776@uga.edu (A.V.); madil@augusta.edu (M.S.A.); malfarhan@augusta.edu (M.A.); sfagan@augusta.edu (S.C.F.); sshenoy@augusta.edu (P.R.S.)
² Charlie Norwood VA Medical Center, Augusta, GA 30912, USA
³ Culver Vision Discovery Institute, Augusta University, Augusta, GA 30912, USA
 * Correspondence: pnarayanan@augusta.edu

Abstract: Visual dysfunction resulting from optic neuritis (ON) is one of the most common clinical manifestations of multiple sclerosis (MS), characterized by loss of retinal ganglion cells, thinning of the nerve fiber layer, and inflammation to the optic nerve. Current treatments available for ON or MS are only partially effective, specifically target the inflammatory phase, and have limited effects on long-term disability. Fingolimod (FTY) is an FDA-approved immunomodulatory agent for MS therapy. The objective of the current study was to evaluate the neuroprotective properties of FTY in the cellular model of ON-associated neuronal damage. R28 retinal neuronal cell damage was induced through treatment with tumor necrosis factor- α (TNF α). In our cell viability analysis, FTY treatment showed significantly reduced TNF α -induced neuronal death. Treatment with FTY attenuated the TNF α -induced changes in cell survival and cell stress signaling molecules. Furthermore, immunofluorescence studies performed using various markers indicated that FTY treatment protects the R28 cells against the TNF α -induced neurodegenerative changes by suppressing reactive oxygen species generation and promoting the expression of neuronal markers. In conclusion, our study suggests neuroprotective effects of FTY in an in vitro model of optic neuritis.

Keywords: optic neuritis; multiple sclerosis; oxidative stress; neuroprotection; fingolimod



Citation: Candadai, A.A.; Liu, F.; Verma, A.; Adil, M.S.; Alfarhan, M.; Fagan, S.C.; Somanath, P.R.; Narayanan, S.P. Neuroprotective Effects of Fingolimod in a Cellular Model of Optic Neuritis. *Cells* **2021**, *10*, 2938. <https://doi.org/10.3390/cells10112938>

Academic Editors: Maurice Ptito and Joseph Bouskila

Received: 10 September 2021
 Accepted: 21 October 2021
 Published: 28 October 2021

Publisher's Note: MDPI stays neutral with regard to jurisdictional claims in published maps and institutional affiliations.



Copyright: © 2021 by the authors. Licensee MDPI, Basel, Switzerland. This article is an open access article distributed under the terms and conditions of the Creative Commons Attribution (CC BY) license (<https://creativecommons.org/licenses/by/4.0/>).

1. Introduction

Multiple sclerosis (MS) is an autoimmune disease of the central nervous system (CNS) prevalent in about 400,000 people in the US and 2.1 million people worldwide [1–4]. Approximately 20% of MS patients present with vision deficits associated with optic neuritis (ON) [5,6], and neurodegeneration characterized by loss of retinal ganglion cells, thinning of the nerve fiber layer, and axonal damage [7,8]. Parameters of visual function are utilized as necessary outcome measures in MS studies [9]. Although the current MS therapies target the inflammatory pathology, effects on the long-term neurodegenerative phases of the disease have not been shown. A treatment that effectively targets both aspects of MS would likely achieve preferred status as a disease-modifying agent.

Fingolimod (FTY720 or FTY), a sphingosine analog that functions as a potent immunosuppressive agent in the CNS, is approved for MS therapy, especially for highly active disease [10,11]. Once phosphorylated into its active form by the sphingosine-1-kinase, it acts as an agonist on sphingosine-1-phosphate (S1P) receptors [12–15] and induces internalization of S1P receptors after binding [16]. Pharmacologically FTY is known as an immunomodulatory drug. FTY exerts its immunosuppressive effect by lymphocyte sequestration and thus reduces the numbers of T and B cells in circulation [17,18]. FTY has been shown to exhibit neuroprotective properties in experimental models of Alzheimer's, stroke,

and Parkinson's disease [19–24]. A recent study showed that FTY exerts neuroprotective and anti-inflammatory effects on the retina and optic nerve in a mouse model of MS, perhaps explaining the potent protective effects in patients [25]. However, the molecular mechanisms regulating the neuroprotective properties have not been studied in retinal neurons. The current study was performed to assess the neuroprotective potential of FTY in an in vitro model of optic neuritis.

The R28 rat neuro-retinal cell line treated with TNF α was standardized to mimic MS-mediated neuronal injury in vitro. The cellular model was chosen based on the studies by Seigel et al. demonstrating the activity and/or expression of neuronal markers at the mRNA, protein, and functional levels in response to various stimuli [26,27]. The expression of neuron-specific markers such as microtubule associated protein 2 (MAP2), Syntaxin, neuron-specific enolase [NSE], Nestin, and receptors for neurotransmitters such as dopamine, serotonin, acetylcholine, and glycine justify the use of these cells to study CNS function [28]. Utilizing the in vitro experimental model of optic neuritis standardized in our laboratory using the tumor necrosis factor- α (TNF α) as an insult, the current study investigated the neuroprotective properties of FTY in reducing the TNF α -induced injury in R28 cells.

2. Materials and Methods

2.1. Cell Culture

Immortalized R28 postnatal day 6 rat neuro-retinal cells (heterogeneous population of cells derived from the parent cell line) (Cat # E1A-NR.3, Kerofast, Inc., Boston, MA, USA) were maintained in low-glucose DMEM medium (Cat # SH30021.01, Hyclone, Logan, UT, USA) supplemented with 10% fetal calf serum (Cat # SH30073.02, Hyclone, Logan, UT, USA), 0.225% Sodium bicarbonate (Cat # S8761, Sigma, St. Louis, MO, USA), 1X MEM non-essential amino acids (Cat # 11140-050, GIBCO, Waltham, MA, USA), 1X MEM vitamins (Cat # 11120-052, GIBCO, Waltham, MA, USA), 0.5 mM l-glutamine (Cat # 25030-081, GIBCO, Waltham, MA, USA), and 50 μ g gentamicin (Cat # 15750-060, GIBCO, Waltham, MA, USA). The cells were differentiated to a neuronal phenotype with the help of 25 μ g/mL laminin (Cat # 11243217001, Sigma, St. Louis, MO, USA) and 250 mM modified cyclic adenosine monophosphate (pCPT-cAMP) (Cat # C3912, Sigma, St. Louis, MO, USA) treatments, according to the published methods [29,30]. All other chemicals were purchased from Fisher Scientific, Waltham, MA, USA, unless otherwise mentioned.

2.2. The In Vitro Model of Optic Neuritis

Dose-response experiments were conducted to standardize the in vitro treatment with TNF α (recombinant rat tumor necrosis factor- α) (Cat # 510-RT, R&D Systems, Minneapolis, MN, USA) to induce neuronal injury in R28 cells. On day 0, cells were differentiated on 6-well culture plates (24 h), as described above. Treatments with TNF α at doses of 5, 10, 25, 50 ng/mL were initiated on day 1, followed by a 24 h incubation period. Cell viability with various doses of TNF α was compared against the control group with no treatment that depicted average growth and differentiation.

2.3. Treatments with Fingolimod

Once the effective dose of TNF α was established, experiments were conducted to identify an appropriate treatment concentration of FTY (Cat # 11975, Cayman Chemicals, Ann Arbor, MI, USA). Cells were pre-treated with FTY at concentrations of 2.5, 5, 10, 25, 50, and 100 nM for a 1 h incubation period before the TNF α treatment. Cell viability differences were compared among control (no treatment), TNF α -treated group, and TNF α co-incubated with varying FTY concentrations. FTY treatment alone at higher doses of 100, 200, and 500 nM were performed to test its cytotoxicity.

2.4. Cell Viability

The degree of viability of R28 cells post-treatment with TNF α and/or FTY was determined using the Trypan blue method [31]. Cells were seeded on six well plates at a density of 0.5×10^6 per well. Following treatments, they were trypsinized and collected in labeled tubes respective to their grouping. Equal volumes of a sample of cell suspension and trypan blue dye were thoroughly mixed using a micropipette, from which 10 μ L was injected into a cell counting chamber (Cat # 02-671-55A, Fischer Scientific, Waltham, MA, USA) for manual counting. Trypan blue dye stains dead cells blue, and the number of viable cells in all four 16-squared tiles of the chamber were counted. This was repeated in triplicates for each cell suspension sample, and cell viability was plotted as the percentage with respect to 100% control. All graphs are represented as Mean \pm SEM.

2.5. Western Blot Analysis

R28 cells seeded at a density of differentiated on six well plates and treated with TNF α and/or FTY as described earlier, resulting in four groups: Control (no treatment), TNF α , TNF α + FTY, and Control + FTY groups. Cells were homogenized, and the lysate was collected in RIPA buffer (Cat # 20-188, EMD Millipore, Burlington, MA, USA) containing protease (Cat # 78430, Fischer Scientific, Waltham, MA, USA) and phosphatase inhibitors (Cat # 78428, Fischer Scientific, Waltham, MA, USA). Protein estimation was performed using the Bradford's protein assay kit (Cat # 5000201, Bio-Rad Laboratories, Hercules, CA, USA). Samples with an equal amount of protein were prepared by using 4X Laemmli buffer (Cat # 161-0747, Bio-Rad Laboratories, Hercules, CA, USA) containing β -mercaptoethanol (Cat # O3446I-100, Fischer Scientific, Waltham, MA, USA). Samples were separated on SDS-PAGE and transferred to nitrocellulose membranes (Cat # 1620112, Bio-Rad Laboratories, Hercules, CA, USA). Membranes were blocked in 5% milk (Cat # 1706404, Bio-Rad Laboratories, Hercules, CA, USA) in tris-buffered saline with tween-20 (TBS-T) and incubated with respective primary antibodies (Table A1) overnight at 4 $^{\circ}$ C. Membranes were washed with 1 \times TBS-T and incubated in appropriate secondary antibodies. Signals were detected using enhanced chemiluminescence (ECL) (Cat # 32106, Fischer Scientific, Waltham, MA, USA). NIH Image J software was utilized to conduct densitometric analysis, and the intensity measurements were normalized to loading control. Experiments were repeated for a minimum of three times.

2.6. Immunofluorescence Staining

Cells seeded at a density of 15,000 to 20,000 cells per well on 8 well glass chamber slides (Cat # 154941, Fischer Scientific, Waltham, MA, USA) were treated according to the study design described previously. Following the 24 h incubation period, the culture media was removed, cells were washed with 1 \times PBS and fixed with 2% paraformaldehyde for 10 min. This was followed by a wash with PBS, and the chamber slides were stored in humidified containers at 4 $^{\circ}$ C. Slides were brought to room temperature and washed with PBS before initiating the staining protocol. Permeabilization was achieved using 0.1% Triton X-100 in PBS for 5 min, followed by a PBS wash, and blocking with 10% donkey serum at room temperature for 1 h. Cells were washed and incubated with respective primary antibodies (Table A1) overnight. The next day, the cells were incubated with appropriate secondary antibodies for 2 h. The Slides were washed, and the chambers were separated from the glass slide. Cells were covered with a coverslip using a mounting medium containing DAPI and stored in 4 $^{\circ}$ C. Images were taken using a confocal microscope (LSM 780; Carl Zeiss, Thornwood, NY, USA) available at the Augusta University imaging core facility. For the Tuj1 and NSE quantitative analysis, similar thresholds were set for all the images. Three to five regions of interest (ROI) were randomly selected per chamber slide images, and the fluorescent intensity of immunoreactivity was measured (Integrated Density) using NIH Image J software. Along with the average fluorescence intensities of a given ROI, the average fluorescence intensity of areas without staining (background) was measured as well. The Corrected Fluorescence was calculated as Integrated Density—(Area of selected

cells X Mean fluorescence of background readings). The values were then normalized relative to percentage of control group. Experiments were repeated a minimum of three times and details are provided under figure legends.

2.7. Cellular ROS Formation Using DCF Assay

CM-H2DCFDA (General Oxidative Stress Indicator, ThermoFisher Scientific, cat# C6827) was used to measure reactive oxygen species (ROS) formation in TNF α treated cells and any changes in response to FTY treatment, as per the manufacturer's instructions. Briefly, cells were washed with ice-cold PBS (three times), and then incubated with 10 μ M CM-H2DCFDA (working solution) at 37 °C for 30 min under dark. Washed with ice-cold PBS (three times), cover-slipped using the mounting medium with DAPI stain (Vector laboratories), and the images were immediately taken by confocal microscope (LSM 780; Carl Zeiss, Thornwood, NY, USA). NIH Image J software was used for the analysis of fluorescent intensity. For single-cell quantification, single-cell was delineated and sampled at 40 \times from a random start point. Only cells with precise neuronal shape and specific nuclear staining with DAPI were analyzed. Three to five chamber slides per treatment were examined and the experiments were repeated three times.

2.8. Mitochondrial ROS Measurement

The production of superoxide by mitochondria in response to TNF α treatment and the impact of FTY on the mitochondrial ROS generation was measured using the MitoSOXTM Red reagent (Thermo Fisher Scientific, cat# M36008), following the manufacturer's instructions. Briefly, cells on chamber slides were washed with ice-cold PBS (three times), incubated with 5 μ M MitoSOXTM reagent working solution, and incubated for 10 min at 37 °C, protected from light. Chamber slides were then carefully washed with ice-cold PBS (three times), cover slipped, and images were immediately taken by confocal microscope (LSM 780; Carl Zeiss, Thornwood, NY, USA). NIH Image J software was used for the analysis of fluorescent intensity. Three to five chamber slides per treatment were examined and the experiments were repeated three times.

2.9. H₂O₂ Treatment and LDH Assay

Oxidative stress was induced on differentiated R28 cells using H₂O₂ (Sigma, USA) following the method of Song et al. [32] with some minor modifications. Briefly, R28 cells were treated with multiple concentrations of H₂O₂ (0.0, 0.2, 0.4, 0.6, 0.8, 1.0, and 1.5 mM) for 24 h and cellular cytotoxicity was measured. In order to determine the effect of FTY on H₂O₂-induced oxidative stress, cells were pre-treated with 25 nM FTY (as described previously) and changes in cytotoxicity was measured.

Lactate dehydrogenase (LDH) assay was used to determine cellular cytotoxicity. LDH released into the culture media from damaged cells was measured following the manufacturer's instructions (CytoTox 96 non-radioactive cytotoxicity assay kit; Promega Corporation, Madison, WI, USA). The level of LDH release was normalized to the total LDH content following cell lysis in a medium. The absorbance was determined at 490 nm using a Multimode Microplate Reader (Berthold Technologies, Bad Wildbad, Germany). LDH release was expressed as a percentage of the maximum LDH released after cell lysis.

2.10. Statistical Analysis

All statistical analyses were performed with GraphPad Prism 7 (GraphPad Software Inc., La Jolla, CA, USA). Student t-test or Two-way ANOVA followed by Tukey's multiple comparisons test was employed to analyze the groups. A *p* value less than 0.05 was considered as statistically significant. Results are presented as Mean \pm SEM.

3. Results

3.1. Fingolimod Treatment Reduces TNF α -Induced Neuronal Injury

We found that TNF α treatment resulted in a significant reduction ($p < 0.05$) in cell viability at doses of 10 ng/mL ($44.6 \pm 24.8\%$), 25 ng/mL ($39.8 \pm 8.7\%$), and 50 ng/mL ($60.2 \pm 13.0\%$) compared to the untreated control (Figure 1A). Our findings suggested that TNF α at 10 ng/mL desirably reduced the percentage of viable cells by nearly half that of the control group. In the next step, cells were pre-treated with fingolimod at concentrations of 0, 2.5, 5, 10, 25, 50, and 100 nM for 1 h prior to TNF α induction (10 ng/mL). Our results showed that FTY concentrations at 25 nM ($79.7 \pm 17.7\%$) and 50 nM ($71.0 \pm 32.3\%$) significantly prevented the TNF α -induced injury ($p < 0.001$) (Figure 2B). Experiments with high-dose FTY treatment alone resulted in cytotoxicity at doses above 100 nM. Doses of 100, 200, and 500 nM showed a decreasing viable cell count of 14.5×10^4 , 3.5×10^4 , and 2×10^4 , respectively, compared to an average viable cell count of 47.5×10^4 in control cells without FTY treatment (not shown). Based on our findings, 25 nM was chosen as the dose of FTY to be used in further studies (Figure 1C).

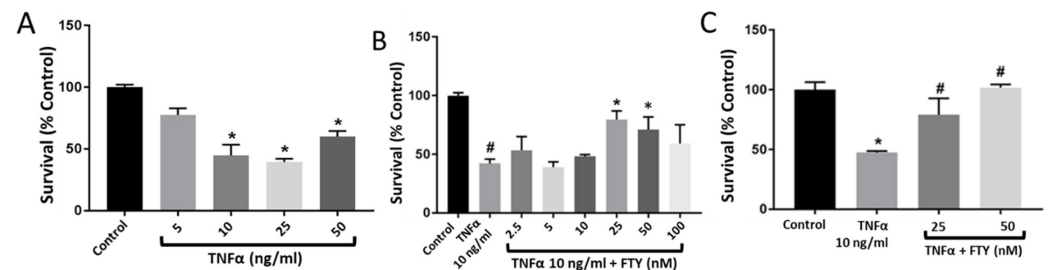


Figure 1. Dose-response effect of TNF α treatment on R28 cell survival and its reversal by co-treatment with fingolimod. (A) Neuronal damage was induced by treating R28 cells with various doses of TNF α for 24 h assessed by Trypan blue method. TNF α at 10 ng/mL showed a marked reduction in cell survival and was chosen as the effective dose for further analysis. [$n = 3$; $* p < 0.05$ vs. dose 0]. (B) Cells were pre-treated with different doses of FTY, followed by TNF α (10 ng/mL), and cell survival was assessed at 24 h. Bar graph showing the effect of 25, 50, and 100 nM FTY on improving the rate of R28 cell survival [$\# p < 0.005$ vs. Con; $* p < 0.05$ vs. TNF α]. (C) Bar graph indicating 25 nM as the optimal dose of FTY in protecting R28 cells from TNF α -induced injury in vitro [$n = 3$; $* p < 0.001$ vs. Con; $\# p < 0.01$ vs. TNF α].

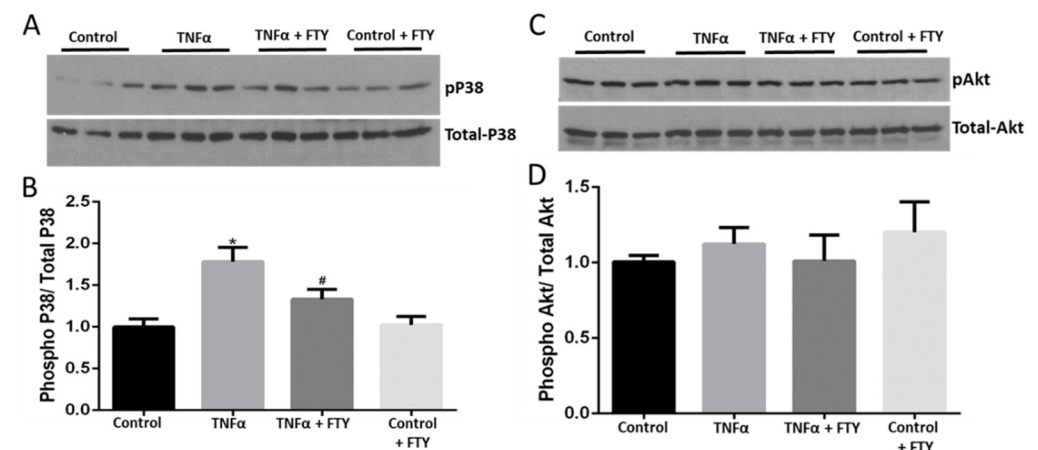


Figure 2. Fingolimod co-treatment mitigates TNF α -induced activation of cellular stress signaling. (A) Western blot images showing upregulation of phospho-p38 MAPK levels in response to TNF α (10 ng/mL) treatment in R28 cells, which was reduced in the presence of FTY. (B) Bar graph showing band densitometry quantification of Western blots indicating the effects of FTY in suppressing P38

MAPK activation induced by TNF α treatment [$n = 6$; * $p < 0.05$ vs. Con; # $p < 0.05$ vs. TNF α]. (C) Western blot images showing no changes in phospho-Akt (Ser473) levels in response to either TNF α (10 ng/mL) and/or FTY in R28 cells. (D) Bar graph showing band densitometry quantification of Western blots indicating the no changes in phospho-Akt (Ser473) levels in response to either TNF α (10 ng/mL) and/or FTY in R28 cells [$n = 6$; NS vs. TNF α].

3.2. Fingolimod Attenuates Cellular Stress and Survival Signaling

Changes in phosphorylated p38 MAP kinase expression were assessed to characterize cellular stress by Western blotting. Figure 2A shows that TNF α augmented the level of p-P38 MAPK, and this increase was markedly prevented in the presence of FTY. Moreover, we found that FTY treatment alone did not affect levels of p-P38 MAPK. Our quantification data demonstrated that in the presence of FTY, levels of p-P38/total-P38 were significantly reduced ($p < 0.05$) versus the TNF α group (Figure 2B). Changes in phosphorylated Akt levels were tested to assess cell survival using Western analysis. Figure 2C shows no changes in the expression of p-AKT with TNF α induction. Consistently, our quantification data also showed no significant decrease in levels of p-Akt/t-Akt in the presence of TNF α versus control (Figure 2D).

3.3. Effect of Fingolimod on Neuronal Cell Death

To evaluate apoptotic changes, Western blot analyses using apoptotic marker cleaved caspase-3, and anti-apoptotic marker Bcl-xL were performed. An upregulated expression on cleaved caspase-3 along with a decreased level of Bcl-xL in the presence of TNF α was observed. In the co-treatment group with TNF α and FTY, we observed a reversal in these changes (Figure 3). Quantification data showed a significant increase in the levels of cleaved caspase-3 ($p < 0.01$) versus control, while FTY treatment significantly reversed this effect ($p < 0.05$) versus the TNF α group (Figure 3B). TNF α caused a significant decrease in levels of Bcl-xL ($p < 0.05$) compared to the control group. However, the difference observed in response to FTY co-treatment was not statistically significant compared to the TNF α group (Figure 3D).

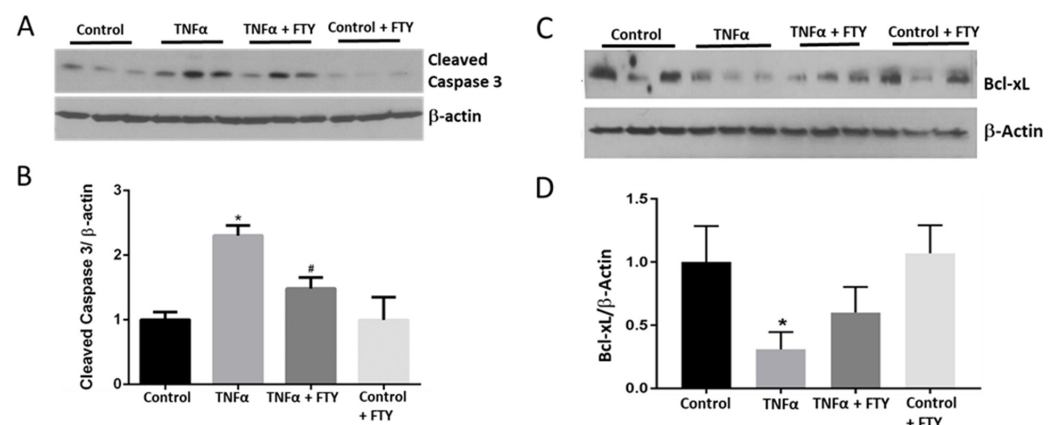


Figure 3. Fingolimod co-treatment blunted TNF α -induced activation of cleaved caspase-3 and expression of Bcl-xL. (A) Representative Western blot data showing increased expression of cleaved caspase-3 with TNF α treatment, which was reduced in the presence of FTY. (B) Bar graph showing band densitometry quantification indicating increased cleaved caspase-3 expression with TNF α treatment [* $p < 0.05$ vs. Con; $n = 3$] and its reversal by co-treatment with FTY [# $p < 0.005$ vs. control; # $p < 0.05$ vs. TNF α ; $n = 4$]. (C) Western blot images showing reduced expression of Bcl-xL with TNF α treatment, which was increased in the presence of FTY. (D) Bar graph showing band densitometry quantification of Western blots indicating reduced Bcl-xL expression with TNF α treatment [* $p < 0.05$, $n = 3$]. The changes observed in response to FTY, however, were not statistically significant.

3.4. Effect of Fingolimod on TNF α -Induced Neuronal Damage

Immunofluorescence studies were conducted to study the neurodegenerative changes observed in R28 cells in response to the different treatments. β -tubulin III, also called Tuj1 contributes to microtubule formation in neuronal cell bodies and axons and plays important roles in axonal transport and cell differentiation. It is a useful marker for the detection of injury-related alterations [33]. Neuron specific enolase (NSE) is widely used and accepted as a neuronal marker, and is expressed by mature neurons and cells of neuronal origin [34]. In the present study, immunostaining with Tuj1 and NSE revealed the degenerative changes induced by TNF α , which was attenuated with FTY treatment (Figure 4A,C). Tuj1 expression was downregulated in TNF α -treated cells; however, we observed that FTY was able to protect the cells against neurofilament damage (Figure 4A lower panels). Consistently, the NSE marker was found to be reduced in the presence of TNF α , and the reduction was prevented by FTY treatment (Figure 4B,D).

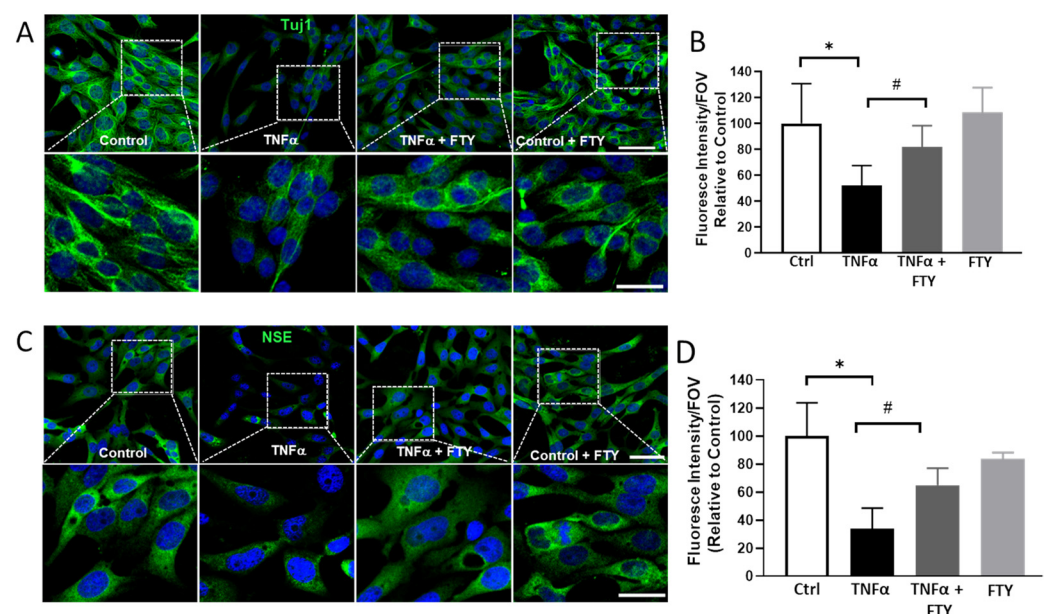


Figure 4. Fingolimod depicts protection against neuronal damage evidenced by immunofluorescence staining of marker proteins. (A) Representative confocal images showing the impact of TNF α treatment on neurofilament, Tuj1 (β -tubulin class III) indicating neurodegeneration, which was reduced by co-treatment with FTY. High magnification images of the boxed areas, indicating reduced Tuj1 expression, are presented in the lower panel. Scale bar 50 μ m. (B) Bar graph showing the quantification of Tuj1 level in response to TNF α treatment, and the protective effect by co-treatment with FTY (C) Representative confocal images showing the changes in neuronal enolase (NSE) in response to TNF α and FTY treatments. Lower panel show high magnification images of the boxed areas, indicating reduced levels in TNF α treated group and the improved NSE expression in response to FTY co-treatment. Scale bar 50 μ m. (D) Bar graph showing the quantification of Tuj1 and NSE levels in response to TNF α treatment, and the effect by co-treatment with FTY [$* p < 0.01$ vs. control; $\# p < 0.01$ vs. TNF α , $n = 3$ per group].

3.5. Effect of Fingolimod on ROS Formation

Changes in ROS formation were studied using DCF assay. As shown in Figure 5A, ROS levels were observed to be markedly elevated in the neuronal cells in response to TNF α treatment. However, treatment with FTY downregulated the TNF α induced ROS generation. Our quantification studies demonstrate that the ROS levels are significantly higher in the TNF α group compared to control and are significantly reduced in response to FTY co-treatment (Figure 5B).

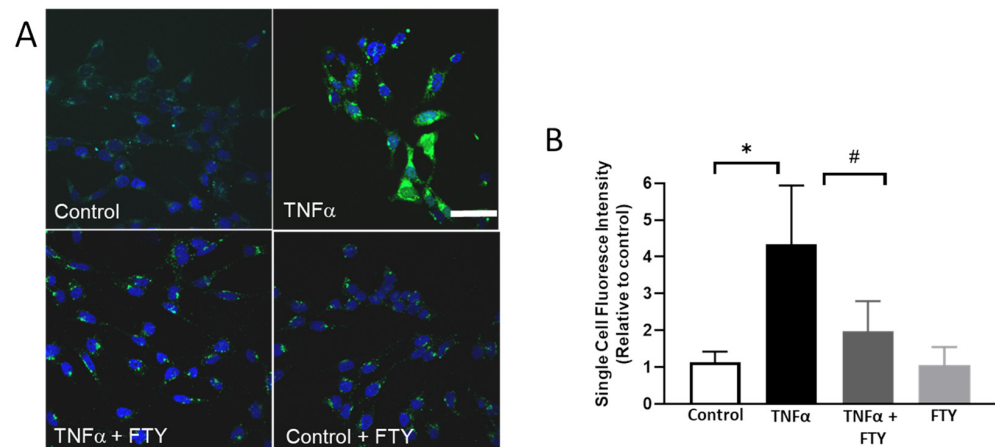


Figure 5. Fingolimod reduced TNF α -induced ROS formation. (A) Representative images showing the impact of FTY on reactive oxygen species (ROS) formation. H2DCFDA (DCF) assay was used to assess the generation of ROS. Scale bar 50 μ m. (B) Quantification of single cell fluorescence intensity showing of the increased ROS formation in response to TNF α treatment, which was reduced in the presence of FTY [$* p < 0.01$ vs. control; $\# p < 0.01$ vs. TNF α , $n = 3$ per group].

3.6. Effect of Fingolimod on Mitochondrial Dynamics and ROS Formation

In the present study, we investigated the effect of FTY treatment on the changes in proteins related to mitochondrial dynamics, including DRP-1 (dynamin related protein-1), Mitofusin 2 and OPA-1 (optic atrophy 1). As illustrated in Figure 6A,D, expression of Mitofusin 2 was significantly reduced in TNF α treated R28 cells, while FTY treatment normalized the level of Mitofusin 2 in TNF α treated cells, similar to control levels. An increase in the level of p-DRP1 was observed in TNF α treated group, while treatment with FTY reversed this effect. However, these changes were not statistically significant. No marked differences were seen in the other mitochondrial proteins studied. Further, we investigated the impact of FTY treatment on mitochondrial ROS formation using MitoSox assay (Figure 6G,H). TNF α treatment resulted in the generation of mitochondrial ROS as evidenced by elevated fluorescence indicator. FTY treatment markedly reduced the level of mitochondrial ROS formed in response to TNF α treatment. Quantification results demonstrate that the mitochondrial ROS level is significantly upregulated in TNF α treated group and the treatment with FTY significantly reduced the effect (Figure 6H).

3.7. Fingolimod Attenuates H₂O₂-Induced Cellular Damage and Stress Signaling in R28 Cells

To further assess the neuroprotective effect of FTY, experiments were performed using H₂O₂, another cellular stressor. Our results show that H₂O₂ induces cytotoxicity in differentiated R28 cells in a dose-dependent manner (Figure 7A). Treatment with FTY significantly reduced the cytotoxicity induced by TNF α at the various concentrations studied (Figure 7B). Our results indicate that H₂O₂ treatments significantly elevated p-P38 levels at all the concentrations studied, while FTY treatment significantly reduced the effect at two different contentions of H₂O₂. FTY treatment did not offer protection at a higher concentration, 1mM of H₂O₂ (Figure 7C).

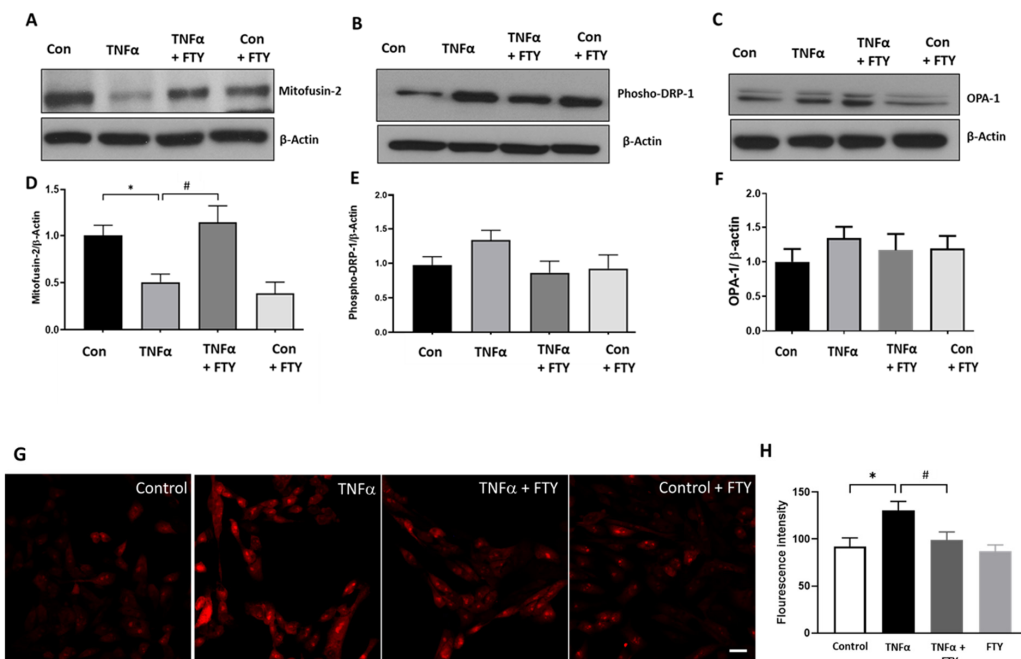


Figure 6. Changes in mitochondrial protein dynamics and ROS formation in response to Fingolimod treatment. (A–C) Representative Western blot data showing changes in expression of proteins associated with mitochondrial dynamics with TNF α treatment, and the effect of FTY cotreatment. (D–F) Respective bar graphs showing quantification of these proteins expression changes with TNF α treatment and any changes by co-treatment with FTY [$* p < 0.05$ vs. control; $\# p < 0.05$ vs. TNF α ; $N = 3$]. (G) Representative images of Mitosox Red staining showing the impact of TNF α on mitochondrial reactive oxygen species (ROS) formation and the effect of FTY on the treatment. Scale bar 20 μ m. (H) Quantification of fluorescence intensity showing of the increased mitochondrial ROS formation in response to TNF α treatment, which was reduced in the presence of FTY [$* p < 0.01$ vs. control; $\# p < 0.01$ vs. TNF α , $n = 3$ per group].

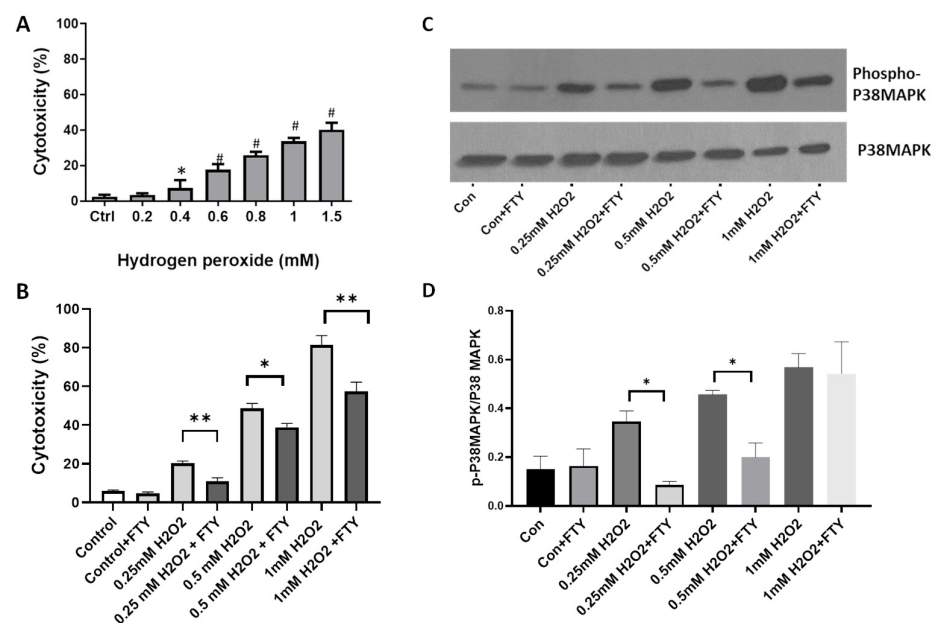


Figure 7. Fingolimod attenuates H₂O₂-induced cellular damage and stress signaling in R28 cells. (A) LDH assay results showing the dose-dependent effect of H₂O₂ treatment on R28 cells. $* p < 0.05$ vs control; $\# p < 0.01$ vs. control and $n = 3$. (B) LDH assay showing the cytotoxic effect of H₂O₂ at

selected concentrations on R28 cells and the protective effect of FTY on the treatments. * $p < 0.05$; ** $p < 0.01$. (C) Representative Western blot data showing changes in p-P38 MAPK with H₂O₂ treatment, and the protective effect of FTY co-treatment on differentiated R28 cells. (D) Bar graph showing quantification of p-P38MAPK proteins expression changes with H₂O₂ and FTY treatments. * $p < 0.01$ and the experiment was repeated three times.

4. Discussion

The present study was conducted to assess the potential neuroprotective action of FTY in an in vitro model of optic neuritis. Lack of effective treatment strategies to reduce neurodegeneration continues to be a major problem in the field of MS research. It is vital to understand the underlying mechanisms of MS-induced neuronal damage and dysfunction. Even though MS research on the pathophysiology and associated molecular mechanisms have evolved over decades of research, including our laboratory [35,36], the field lacks reliable in vitro models to study neurodegeneration. Synthetic molecules such as trimethyltin [37], oxaliplatin [38], and cuprizone [39], although successful in creating a neurodegenerative environment, do not accurately represent the neuroinflammatory changes observed in an MS brain. In MS, inflammatory leukocytes are believed to infiltrate the CNS to mediate demyelination and neuronal degeneration via cytokines upon activation of T lymphocytes and antigen-presenting cells (APCs) [40]. tumor necrosis factor- α (TNF α) is one of the primary cytokines that are present in elevated levels in active MS lesions, serum, and cerebrospinal fluid of MS patients [41]. Studies conducted on BV-2 microglial cell lines [42] and primary mixed neuronal and glial cultures [43] show the effect of TNF α -induced damage and apoptosis. Hence, utilizing the R28 neuro-retinal cells, we standardized an in vitro experimental model of neurodegeneration to assess the impact of fingolimod on TNF α -induced neuronal damage. Using a set of functional and biochemical analyses, our study demonstrates the neuroprotective properties of fingolimod in MS-associated optic neuritis in vitro.

We first demonstrated the dose-dependent effects of TNF α on neuronal cell viability in R28 neuro-retinal cells in vitro and identified the optimal dose of TNF α for further molecular characterization. The R28 cells are immortalized, rat retinal origin, heterogenous, precursor cells with differentiation potential [26]. According to the published methods, R28 cells were differentiated to neuronal phenotype with the addition of a modified form of cAMP and laminin and grown using DMEM [44–46]. Studies by Seigel et al. utilizing R28 cells demonstrate the expression of neuron-specific markers such as MAP2, Syntaxin, NSE, and Nestin, along with neurotransmission receptors [26,28]. Our study characterized the expression of neurofilament marker Tuj1, along with NSE in these cells, thus demonstrating the reliability of this model in evaluating the impact of FTY on the neuronal injury. In MS, one of the major clinical presentations observed in patients is optic neuritis [47]. Studies have shown that approximately 20% of patients present with inflammation of the optic nerve as their first symptom of MS [5,6]. Another study conducted by the North American Research Committee on multiple sclerosis (NARCOMS) showed that of the 9107 patients participating in the study, 60% reported signs of vision impairment, and 14% of these depicted moderate/severe/very severe impairment of vision [9]. Based on the available research, visual dysfunction is a common component of MS disease progression and an important determinant of quality of life.

Current MS therapies function by suppressing the inflammatory pathways and have unknown impact on the long-term neuronal damage, causing a major knowledge gap and emphasizes the need to identify a neuroprotective therapeutic agent. Therefore, our study focused on assessing the neuroprotective effect of FTY in an in vitro model of MS-induced optic neuritis. Fingolimod, a sphingosine-1-phosphate (S1P) receptor modulator, has previously been shown to prevent neurodegenerative mechanisms targeting an inflammatory CNS state in vitro, in vivo, and clinical settings, as detailed below. Studies on Parkinson's disease models have shown a positive impact with FTY [19–21]. Mechanistically, it was found that the protective effects of FTY in Parkinson's disease were correlated with the activation of survival pathway mediated by Akt/ERK1/2 and increased expression of a

neuron-specific brain-derived neurotrophic factor (BDNF). In a model of Alzheimer's, FTY was able to reverse the effect of damage by modulating the levels of different markers such as the Glial fibrillary acidic protein (astroglial marker), taurine (anti-inflammatory marker), and neuronal markers such as the N-acetyl aspartate and glutamate [23]. A meta-analysis was conducted by Liu et al. which included nine studies that focused on quantification of infarct volume and neurological deficit scoring in a transient middle cerebral artery occlusion model of ischemic stroke challenged with FTY [24]. The study concluded that FTY could be a possible candidate for stroke due to its protective effects on neurological deficit and infarct volume in eight of the nine included studies. Promising outcomes with FTY represent the need for further investigation to confirm the theories on its action as a neuroprotective agent. Utilizing the EAE (Experimental Autoimmune Encephalitis) model of MS, a recent study by Yang et al. investigated whether FTY is beneficial to the visual system [25]. Their results showed that FTY treatment offered neuroprotective and anti-inflammatory effects on the retina and optic nerve. FTY treatment alleviated EAE-induced gliosis, inflammation and reduced the apoptosis of RGCs and oligodendrocytes.

In response to FTY treatment, our studies found a reduction in the phosphorylation of p38 MAP kinase (a cellular stress signaling pathway) in TNF α -treated R28 cells. However, fingolimod treatment did not induce any changes in the levels of phosphorylated Akt, indicating its effect on cell survival is independent of Akt, with the conditions studied. TNF α -induced cell death was confirmed by the upregulation of cleaved caspase-3 (a cell death marker) expression along with reduced levels of Bcl-xL (an anti-apoptotic protein). These changes were reversed in response to FTY treatment, supporting its neuroprotective and anti-apoptotic function. FTY treatment also protected the retinal neurons against the TNF α -induced neuronal damage determined by the expression of neuronal markers.

Oxidative stress plays a critical part in the pathogenesis of various neurodegenerative diseases and neuroinflammation. There exists an increasing amount of data indicating that oxidative stress plays a major role in the pathogenesis of MS and optic neuritis [48]. Results from preclinical studies show that suppression of oxidative stress is a promising strategy for optic neuritis [49–53]. In the present study, we show that FTY mediated neuroprotection of R28 cells involves the regulation of ROS formation. A recent study performed on serum samples from patients with relapsing-remitting MS and healthy controls demonstrated that FTY treatment increased total antioxidant capacity [54]. Furthermore, FTY treatment reduced oxidative stress in experimental models of cardiomyopathy [55], multiple system atrophy [56], autism [57], and vitamin K-induced neurotoxicity [20].

Oxidative damages along with mitochondrial dysfunction are common characteristics of neurodegenerative diseases. Mitochondrial dysfunction is increasingly recognized as a major mechanism of MS associated pathologies [58–60]. The present study investigated the impact of FTY treatment on the changes in protein levels related to mitochondrial dynamics. Alterations in mitochondrial dynamics affect mitochondrial size and shape and impact mitochondrial metabolism and cell death. These events are controlled by mitochondrial dynamin-related GTPases, including mitofusin-1, mitofusin-2, OPA1, and DRP1. Our results show that one possible mechanism by which FTY offers neuroprotection of R28 neuronal cells via regulation of mitochondrial fusion. Altered levels of mitochondrial proteins were reported in retinal neurons in models of diabetic retinopathy [61] and glaucoma [62]. Results from our study are consistent with studies on neuroprotective properties of FTY in other models where FTY improved mitochondrial stability and restored mitochondrial dynamics under oxidative stress conditions [20,63–65]. Our present study did not investigate the changes in mitochondrial function.

Our study showed that FTY treatment reduces TNF α induced mitochondrial ROS formation in R28 cells. Other studies recently reported that FTY reduced mitochondrial dysfunction in a rat model of chronic cerebral hypoperfusion, reduced neuroinflammation and restored mitochondrial function in a model of Multiple System Atrophy [65], prevented mitochondrial dysfunction and protected neurons in prion protein-disease model [66].

Furthermore, we investigated the neuroprotective effect of FTY on R28 cells treated with H_2O_2 , a cellular stressor known to induce oxidative stress. Our results reveal that FTY offers neuroprotection in response to oxidative stress-induced cellular damage. While FTY treatment rescued R28 cells at all concentrations of H_2O_2 studied, FTY did not significantly reduce phospho-P38 levels at higher concentration of H_2O_2 , suggesting the possibility of other signaling pathways involved. Another possibility is that FTY at a different dose/time could reduce the phospho-P38 levels at higher concentrations of H_2O_2 . Overall, these results indicate that FTY mediated neuroprotection could be offered through multiple mechanisms, including P38MAPK signaling. However, further studies are needed to confirm this observation.

Evidence as a regulator of oxidative stress, along with its immunomodulatory function, offers significant therapeutic potential to FTY in neuroinflammatory diseases such as optic neuritis. Figure 8 depicts the possible mechanisms of FTY mediated neuroprotection in response to $TNF\alpha$ -induced damage. Further studies are needed to define whether the effect of FTY on ROS level is direct or indirect and to delineate the molecular mechanisms of FTY mediated neuroprotection.

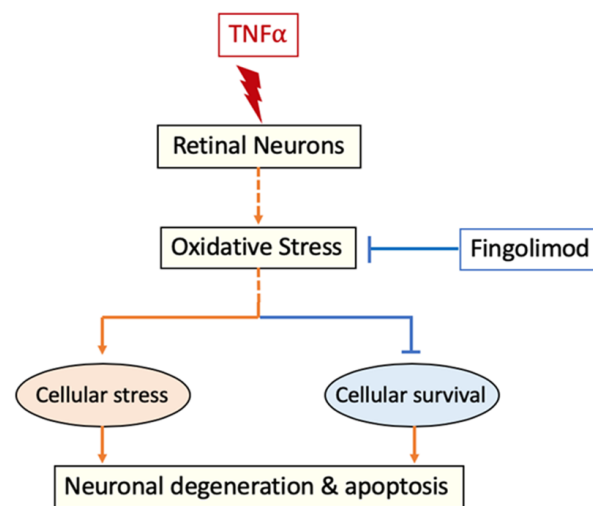


Figure 8. Proposed mechanism of FTY mediated neuroprotection. It is postulated that $TNF\alpha$ treatment induces cellular stress and cell death in retinal neurons by elevating oxidative stress. Treatment with FTY reduces $TNF\alpha$ -induced oxidative stress and improved neuronal survival.

One limitation of our study is that it did not elucidate the role of cell survival pathways that are directly associated with $TNF\alpha$ and FTY action. The concentration of FTY used in our study (25 nM) corresponds to 7.6875 ng/mL. However, as per the manufacturer's (Gilenya®) package insert, the concentration of active fingolimod phosphate in adult MS patients is 1.35 ng/mL. Lower concentrations used in our study, did not offer any neuroprotective effect. It is likely that the neurovascular unit could respond differently in response to other cytokines or injury mediators. This difference in human systemic concentration versus in vitro concentration in our models is an interesting aspect of the study and suggests that repurposing may be needed for the neuroprotective action of FTY in MS patients. Another limitation of the current study is that it is purely performed in a cellular model in vitro, which is not a true reflection of what happens in a complex in vivo set up. Nevertheless, the study provides reasonable optimism on the potential therapeutic benefits of FTY to treat ON. Studies performed on EAE model by Yang et al demonstrated neuroprotective and anti-inflammatory effects on the retina and optic nerve, with no direct negative effects at the two different doses of FTY (0.3 and 1.0 mg/kg) utilized [25]. Results from our study complements the findings of Yang et al., where stronger neuroprotective effects on the visual system.

5. Conclusions

Overall, our study investigated the potential neuroprotective effects of FTY in an in vitro model of neurodegeneration. The R28 neuro-retinal cells are characterized as a successful platform for evaluating neuronal damage in the presence of TNF α , and its suppression with FTY. Furthermore, our studies demonstrated the antioxidant properties of FTY, a possible mechanism of neuroprotection. However, further studies are required to confirm the results. Based on the cellular and molecular analysis, FTY demonstrated the potential to be investigated as a novel neuroprotective strategy in conditions like MS and associated pathologies.

Author Contributions: Conceptualization, S.P.N. and S.C.F.; methodology, A.A.C., F.L., A.V., M.A. and M.S.A.; formal analysis, A.A.C., F.L., A.V. and M.S.A.; investigation, A.A.C., F.L., A.V. and M.A.; resources, S.P.N. and P.R.S.; writing—original draft preparation, A.A.C.; writing—review and editing, F.L., M.A., M.S.A., S.C.F., P.R.S. and S.P.N.; supervision, S.P.N.; project administration, S.P.N.; funding acquisition, S.P.N. All authors have read and agreed to the published version of the manuscript.

Funding: This study was supported in part by University of Georgia startup funds and the National Eye Institute to SPN (R01EY028569). This work has been accomplished using the resources and facilities at the Charlie Norwood VA Medical Center, Augusta, GA, and a core grant from the NIH/NEI to the Augusta University Vision Discovery Institute (P30EY031631). The funders had no role in study design, data collection, analysis, and decision to publish the data. The contents of the manuscript do not represent the views of the Department of Veteran Affairs or the United States.

Institutional Review Board Statement: Not applicable.

Informed Consent Statement: Not applicable.

Data Availability Statement: Not applicable.

Acknowledgments: The authors are thankful to Chithra Palani for her assistance with the R28 cell culture studies.

Conflicts of Interest: The authors declare no conflict of interest.

Appendix A

Table A1. List of antibodies used in the study.

Antibody Used	Catalogue No.	Company	Dilution
Phospho-P38 MAP Kinase	4511S	Cell Signaling	1:1000
Total P38 MAP Kinase	9212S	Cell Signaling	1:1000
Phospho-Akt	4060S	Cell Signaling	1:1000
Total Akt	9272S	Cell Signaling	1:1000
Bcl-xL	2764S	Cell Signaling	1:1000
Cleaved caspase-3	9664S	Cell Signaling	1:1000
β -Actin	A1978-200UL	Sigma	1:10,000
Tuj1	MAB1195	R&D Systems	1:500
Neuron Specific Enolase	NSE	Aves Lab	1:500
Mitofusin-2	74792	Cell Signaling	1:1000
p-DRP-1	4494	Cell Signaling	1:1000
OPA-1	80471S	Cell Signaling	1:1000

References

1. Filippi, M.; Rocca, M.A. Multiple sclerosis: New measures to monitor the disease. *Lancet Neurol.* **2013**, *12*, 12–13. [[CrossRef](#)]
2. Lassmann, H.; van Horssen, J. The molecular basis of neurodegeneration in multiple sclerosis. *FEBS Lett.* **2011**, *585*, 3715–3723. [[CrossRef](#)]
3. Zwibel, H.L.; Smrtka, J. Improving quality of life in multiple sclerosis: An unmet need. *Am. J. Manag. Care* **2011**, *17* (Suppl. 5), S139–S145. [[PubMed](#)]
4. Waubant, E.; Lucas, R.; Mowry, E.; Graves, J.; Olsson, T.; Alfredsson, L.; Langer-Gould, A. Environmental and genetic risk factors for MS: An integrated review. *Ann. Clin. Transl. Neurol.* **2019**, *6*, 1905–1922. [[CrossRef](#)] [[PubMed](#)]
5. Burman, J.; Raininko, R.; Fagius, J. Bilateral and recurrent optic neuritis in multiple sclerosis. *Acta Neurol. Scand.* **2011**, *123*, 207–210. [[CrossRef](#)] [[PubMed](#)]
6. Sorensen, T.L.; Frederiksen, J.L.; Bronnum-Hansen, H.; Petersen, H.C. Optic neuritis as onset manifestation of multiple sclerosis: A nationwide, long-term survey. *Neurology* **1999**, *53*, 473–478. [[CrossRef](#)] [[PubMed](#)]
7. Walter, S.D.; Ishikawa, H.; Galetta, K.M.; Sakai, R.E.; Feller, D.J.; Henderson, S.B.; Wilson, J.A.; Maguire, M.G.; Galetta, S.L.; Frohman, E.; et al. Ganglion cell loss in relation to visual disability in multiple sclerosis. *Ophthalmology* **2012**, *119*, 1250–1257. [[CrossRef](#)]
8. Trip, S.A.; Schlottmann, P.G.; Jones, S.J.; Altmann, D.R.; Garway-Heath, D.F.; Thompson, A.J.; Plant, G.T.; Miller, D.H. Retinal nerve fiber layer axonal loss and visual dysfunction in optic neuritis. *Ann. Neurol.* **2005**, *58*, 383–391. [[CrossRef](#)]
9. Salter, A.R.; Tyry, T.; Vollmer, T.; Cutter, G.R.; Marrie, R.A. “Seeing” in NARCOMS: A look at vision-related quality of life in the NARCOMS registry. *Mult. Scler.* **2013**, *19*, 953–960. [[CrossRef](#)]
10. Adachi, K.; Chiba, K. FTY720 story. Its discovery and the following accelerated development of sphingosine 1-phosphate receptor agonists as immunomodulators based on reverse pharmacology. *Perspect. Med. Chem.* **2007**, *1*, 11–23. [[CrossRef](#)]
11. Park, S.J.; Im, D.S. Sphingosine 1-Phosphate Receptor Modulators and Drug Discovery. *Biomol. Ther. (Seoul)* **2017**, *25*, 80–90. [[CrossRef](#)]
12. Brinkmann, V.; Billich, A.; Baumruker, T.; Heining, P.; Schmouder, R.; Francis, G.; Aradhye, S.; Burtin, P. Fingolimod (FTY720): Discovery and development of an oral drug to treat multiple sclerosis. *Nat. Rev. Drug Discov.* **2010**, *9*, 883–897. [[CrossRef](#)]
13. Brinkmann, V.; Davis, M.D.; Heise, C.E.; Albert, R.; Cottens, S.; Hof, R.; Bruns, C.; Prieschl, E.; Baumruker, T.; Hiestand, P.; et al. The immune modulator FTY720 targets sphingosine 1-phosphate receptors. *J. Biol. Chem.* **2002**, *277*, 21453–21457. [[CrossRef](#)]
14. Dyckman, A.J. Modulators of Sphingosine-1-phosphate Pathway Biology: Recent Advances of Sphingosine-1-phosphate Receptor 1 (S1P1) Agonists and Future Perspectives. *J. Med. Chem.* **2017**, *60*, 5267–5289. [[CrossRef](#)] [[PubMed](#)]
15. Miron, V.E.; Schubart, A.; Antel, J.P. Central nervous system-directed effects of FTY720 (fingolimod). *J. Neurol. Sci.* **2008**, *274*, 13–17. [[CrossRef](#)]
16. Matloubian, M.; Lo, C.G.; Cinamon, G.; Lesneski, M.J.; Xu, Y.; Brinkmann, V.; Allende, M.L.; Proia, R.L.; Cyster, J.G. Lymphocyte egress from thymus and peripheral lymphoid organs is dependent on S1P receptor 1. *Nature* **2004**, *427*, 355–360. [[CrossRef](#)] [[PubMed](#)]
17. Graler, M.H.; Goetzl, E.J. The immunosuppressant FTY720 down-regulates sphingosine 1-phosphate G-protein-coupled receptors. *FASEB J.* **2004**, *18*, 551–553. [[CrossRef](#)] [[PubMed](#)]
18. Chiba, K.; Yanagawa, Y.; Masubuchi, Y.; Kataoka, H.; Kawaguchi, T.; Ohtsuki, M.; Hoshino, Y. FTY720, a novel immunosuppressant, induces sequestration of circulating mature lymphocytes by acceleration of lymphocyte homing in rats. I. FTY720 selectively decreases the number of circulating mature lymphocytes by acceleration of lymphocyte homing. *J. Immunol.* **1998**, *160*, 5037–5044.
19. Zhao, P.; Yang, X.; Yang, L.; Li, M.; Wood, K.; Liu, Q.; Zhu, X. Neuroprotective effects of fingolimod in mouse models of Parkinson’s disease. *FASEB J.* **2017**, *31*, 172–179. [[CrossRef](#)]
20. Martin-Montanez, E.; Pavia, J.; Valverde, N.; Boraldi, F.; Lara, E.; Oliver, B.; Hurtado-Guerrero, I.; Fernandez, O.; Garcia-Fernandez, M. The S1P mimetic fingolimod phosphate regulates mitochondrial oxidative stress in neuronal cells. *Free Radic. Biol. Med.* **2019**, *137*, 116–130. [[CrossRef](#)]
21. Ren, M.; Han, M.; Wei, X.; Guo, Y.; Shi, H.; Zhang, X.; Perez, R.G.; Lou, H. FTY720 Attenuates 6-OHDA-Associated Dopaminergic Degeneration in Cellular and Mouse Parkinsonian Models. *Neurochem. Res.* **2017**, *42*, 686–696. [[CrossRef](#)]
22. Vidal-Martinez, G.; Vargas-Medrano, J.; Gil-Tommee, C.; Medina, D.; Garza, N.T.; Yang, B.; Segura-Ulate, I.; Dominguez, S.J.; Perez, R.G. FTY720/Fingolimod Reduces Synucleinopathy and Improves Gut Motility in A53T Mice: Contributions of pro-brain-derived neurotrophic factor (pro-bdnf) and mature bdnf. *J. Biol. Chem.* **2016**, *291*, 20811–20821. [[CrossRef](#)]
23. Aytan, N.; Choi, J.K.; Carreras, I.; Brinkmann, V.; Kowall, N.W.; Jenkins, B.G.; Dedeoglu, A. Fingolimod modulates multiple neuroinflammatory markers in a mouse model of Alzheimer’s disease. *Sci. Rep.* **2016**, *6*, 24939. [[CrossRef](#)] [[PubMed](#)]
24. Liu, J.; Zhang, C.; Tao, W.; Liu, M. Systematic review and meta-analysis of the efficacy of sphingosine-1-phosphate (S1P) receptor agonist FTY720 (fingolimod) in animal models of stroke. *Int. J. Neurosci.* **2013**, *123*, 163–169. [[CrossRef](#)]
25. Yang, T.; Zha, Z.; Yang, X.; Kang, Y.; Wang, X.; Tong, Y.; Zhao, X.; Wang, L.; Fan, Y. Neuroprotective Effects of Fingolimod Supplement on the Retina and Optic Nerve in the Mouse Model of Experimental Autoimmune Encephalomyelitis. *Front. Neurosci.* **2021**, *15*, 663541. [[CrossRef](#)] [[PubMed](#)]
26. Seigel, G.M. Review: R28 retinal precursor cells: The first 20 years. *Mol. Vis.* **2014**, *20*, 301–306. [[PubMed](#)]
27. Seigel, G.M.; Mutchler, A.L.; Imperato, E.L. Expression of glial markers in a retinal precursor cell line. *Mol. Vis.* **1996**, *2*, 9233983.

28. Seigel, G.M.; Sun, W.; Wang, J.; Hershberger, D.H.; Campbell, L.M.; Salvi, R.J. Neuronal gene expression and function in the growth-stimulated R28 retinal precursor cell line. *Curr. Eye Res.* **2004**, *28*, 257–269. [[CrossRef](#)]
29. Boriushkin, E.; Wang, J.J.; Li, J.; Jing, G.; Seigel, G.M.; Zhang, S.X. Identification of p58IPK as a novel neuroprotective factor for retinal neurons. *Investig. Ophthalmol. Vis. Sci.* **2015**, *56*, 1374–1386. [[CrossRef](#)]
30. Kong, D.; Gong, L.; Arnold, E.; Shanmugam, S.; Fort, P.E.; Gardner, T.W.; Abcouwer, S.F. Insulin-like growth factor 1 rescues R28 retinal neurons from apoptotic death through ERK-mediated BimEL phosphorylation independent of Akt. *Exp. Eye Res.* **2016**, *151*, 82–95. [[CrossRef](#)]
31. Goc, A.; Kochuparambil, S.T.; Al-Husein, B.; Al-Azayzih, A.; Mohammad, S.; Somanath, P.R. Simultaneous modulation of the intrinsic and extrinsic pathways by simvastatin in mediating prostate cancer cell apoptosis. *BMC Cancer* **2012**, *12*, 409. [[CrossRef](#)] [[PubMed](#)]
32. Song, Y.; Hong, S.; Iizuka, Y.; Kim, C.Y.; Seong, G.J. The neuroprotective effect of maltol against oxidative stress on rat retinal neuronal cells. *Korean J. Ophthalmol.* **2015**, *29*, 58–65. [[CrossRef](#)]
33. Geisert, E.E., Jr.; Frankfurter, A. The neuronal response to injury as visualized by immunostaining of class III beta-tubulin in the rat. *Neurosci. Lett.* **1989**, *102*, 137–141. [[CrossRef](#)]
34. Iwanaga, T.; Takahashi, Y.; Fujita, T. Immunohistochemistry of neuron-specific and glia-specific proteins. *Arch. Histol. Cytol.* **1989**, *52*, 13–24. [[CrossRef](#)]
35. Palani, C.D.; Fouda, A.Y.; Liu, F.; Xu, Z.; Mohamed, E.; Giri, S.; Smith, S.B.; Caldwell, R.B.; Narayanan, S.P. Deletion of Arginase 2 Ameliorates Retinal Neurodegeneration in a Mouse Model of Multiple Sclerosis. *Mol. Neurobiol.* **2019**, *56*, 8589–8602. [[CrossRef](#)] [[PubMed](#)]
36. Candadai, A.A.; Liu, F.; Fouda, A.Y.; Alfarhan, M.; Palani, C.D.; Xu, Z.; Caldwell, R.B.; Narayanan, S.P. Deletion of arginase 2 attenuates neuroinflammation in an experimental model of optic neuritis. *PLoS ONE* **2021**, *16*, e0247901. [[CrossRef](#)]
37. Long, J.; Wang, Q.; He, H.; Sui, X.; Lin, G.; Wang, S.; Yang, J.; You, P.; Luo, Y.; Wang, Y. NLRP3 inflammasome activation is involved in trimethyltin-induced neuroinflammation. *Brain Res.* **2019**, *1718*, 186–193. [[CrossRef](#)]
38. Miyagi, A.; Kawashiri, T.; Shimizu, S.; Shigematsu, N.; Kobayashi, D.; Shimazoe, T. Dimethyl Fumarate Attenuates Oxaliplatin-Induced Peripheral Neuropathy without Affecting the Anti-tumor Activity of Oxaliplatin in Rodents. *Biol. Pharm. Bull.* **2019**, *42*, 638–644. [[CrossRef](#)] [[PubMed](#)]
39. Clarner, T.; Janssen, K.; Nellessen, L.; Stangel, M.; Skripuletz, T.; Krauspe, B.; Hess, F.M.; Denecke, B.; Beutner, C.; Linnartz-Gerlach, B.; et al. CXCL10 triggers early microglial activation in the cuprizone model. *J. Immunol.* **2015**, *194*, 3400–3413. [[CrossRef](#)] [[PubMed](#)]
40. Gobel, K.; Ruck, T.; Meuth, S.G. Cytokine signaling in multiple sclerosis: Lost in translation. *Mult. Scler.* **2018**, *24*, 432–439. [[CrossRef](#)]
41. Sharief, M.K.; Hentges, R. Association between tumor necrosis factor-alpha and disease progression in patients with multiple sclerosis. *N. Engl. J. Med.* **1991**, *325*, 467–472. [[CrossRef](#)]
42. Lei, Q.; Tan, J.; Yi, S.; Wu, N.; Wang, Y.; Wu, H. Mitochondrial acid 5 activates the MAPK-ERK-yap signaling pathways to protect mouse microglial BV-2 cells against TNFalpha-induced apoptosis via increased Bnip3-related mitophagy. *Cell Mol. Biol. Lett.* **2018**, *23*, 14. [[CrossRef](#)]
43. Neniskyte, U.; Vilalta, A.; Brown, G.C. Tumour necrosis factor alpha-induced neuronal loss is mediated by microglial phagocytosis. *FEBS Lett.* **2014**, *588*, 2952–2956. [[CrossRef](#)]
44. Pang, Y.; Qin, M.; Hu, P.; Ji, K.; Xiao, R.; Sun, N.; Pan, X.; Zhang, X. Resveratrol protects retinal ganglion cells against ischemia induced damage by increasing Opa1 expression. *Int. J. Mol. Med.* **2020**, *46*, 1707–1720. [[CrossRef](#)]
45. Mathew, B.; Chennakesavalu, M.; Sharma, M.; Torres, L.A.; Stelman, C.R.; Tran, S.; Patel, R.; Burg, N.; Salkovski, M.; Kadzielawa, K.; et al. Autophagy and post-ischemic conditioning in retinal ischemia. *Autophagy* **2020**, *17*, 1479–1499. [[CrossRef](#)]
46. Tan, J.; Digicaylioglu, M.; Wang, S.X.J.; Dresselhuis, J.; Dedhar, S.; Mills, J. Insulin attenuates apoptosis in neuronal cells by an integrin-linked kinase-dependent mechanism. *Heliyon* **2019**, *5*, e02294. [[CrossRef](#)] [[PubMed](#)]
47. Kale, N. Optic neuritis as an early sign of multiple sclerosis. *Eye Brain* **2016**, *8*, 195–202. [[CrossRef](#)] [[PubMed](#)]
48. Kimura, A.; Namekata, K.; Guo, X.; Noro, T.; Harada, C.; Harada, T. Targeting Oxidative Stress for Treatment of Glaucoma and Optic Neuritis. *Oxidative Med. Cell Longev.* **2017**, *2017*, 2817252. [[CrossRef](#)]
49. Gilgun-Sherki, Y.; Melamed, E.; Offen, D. The role of oxidative stress in the pathogenesis of multiple sclerosis: The need for effective antioxidant therapy. *J. Neurol.* **2004**, *251*, 261–268. [[CrossRef](#)] [[PubMed](#)]
50. Guo, X.; Harada, C.; Namekata, K.; Matsuzawa, A.; Camps, M.; Ji, H.; Swinnen, D.; Jorand-Lebrun, C.; Muzerelle, M.; Vitte, P.A.; et al. Regulation of the severity of neuroinflammation and demyelination by TLR-ASK1-p38 pathway. *EMBO Mol. Med.* **2010**, *2*, 504–515. [[CrossRef](#)]
51. Azuchi, Y.; Kimura, A.; Guo, X.; Akiyama, G.; Noro, T.; Harada, C.; Nishigaki, A.; Namekata, K.; Harada, T. Valproic acid and ASK1 deficiency ameliorate optic neuritis and neurodegeneration in an animal model of multiple sclerosis. *Neurosci. Lett.* **2017**, *639*, 82–87. [[CrossRef](#)]
52. Guo, X.; Harada, C.; Namekata, K.; Kimura, A.; Mitamura, Y.; Yoshida, H.; Matsumoto, Y.; Harada, T. Spermidine alleviates severity of murine experimental autoimmune encephalomyelitis. *Investig. Ophthalmol. Vis. Sci.* **2011**, *52*, 2696–2703. [[CrossRef](#)] [[PubMed](#)]

53. Guo, X.; Namekata, K.; Kimura, A.; Noro, T.; Azuchi, Y.; Semba, K.; Harada, C.; Yoshida, H.; Mitamura, Y.; Harada, T. Brimonidine suppresses loss of retinal neurons and visual function in a murine model of optic neuritis. *Neurosci. Lett.* **2015**, *592*, 27–31. [[CrossRef](#)] [[PubMed](#)]
54. Yevgi, R.; Demir, R. Oxidative stress activity of fingolimod in multiple sclerosis. *Clin. Neurol. Neurosurg.* **2021**, *202*, 106500. [[CrossRef](#)]
55. Ryba, D.M.; Warren, C.M.; Karam, C.N.; Davis, R.T., 3rd; Chowdhury, S.A.K.; Alvarez, M.G.; McCann, M.; Liew, C.W.; Wieczorek, D.F.; Varga, P.; et al. Sphingosine-1-Phosphate Receptor Modulator, FTY720, Improves Diastolic Dysfunction and Partially Reverses Atrial Remodeling in a Tm-E180G Mouse Model Linked to Hypertrophic Cardiomyopathy. *Circ. Heart Fail.* **2019**, *12*, e005835. [[CrossRef](#)] [[PubMed](#)]
56. Vargas-Medrano, J.; Segura-Ulate, I.; Yang, B.; Chinnasamy, R.; Arterburn, J.B.; Perez, R.G. FTY720-Mitoxoy reduces toxicity associated with MSA-like alpha-synuclein and oxidative stress by increasing trophic factor expression and myelin protein in OLN-93 oligodendroglia cell cultures. *Neuropharmacology* **2019**, *158*, 107701. [[CrossRef](#)] [[PubMed](#)]
57. Wu, H.; Wang, X.; Gao, J.; Liang, S.; Hao, Y.; Sun, C.; Xia, W.; Cao, Y.; Wu, L. Fingolimod (FTY720) attenuates social deficits, learning and memory impairments, neuronal loss and neuroinflammation in the rat model of autism. *Life Sci.* **2017**, *173*, 43–54. [[CrossRef](#)]
58. Ng, X.; Sadeghian, M.; Heales, S.; Hargreaves, I.P. Assessment of Mitochondrial Dysfunction in Experimental Autoimmune Encephalomyelitis (EAE) Models of Multiple Sclerosis. *Int. J. Mol. Sci.* **2019**, *20*, 4975. [[CrossRef](#)]
59. Mancini, A.; Tantucci, M.; Mazzocchetti, P.; de Iure, A.; Durante, V.; Macchioni, L.; Giampa, C.; Alvino, A.; Gaetani, L.; Costa, C.; et al. Microglial activation and the nitric oxide/cGMP/PKG pathway underlie enhanced neuronal vulnerability to mitochondrial dysfunction in experimental multiple sclerosis. *Neurobiol. Dis.* **2018**, *113*, 97–108. [[CrossRef](#)]
60. Sadeghian, M.; Mastrolia, V.; Rezaei Haddad, A.; Mosley, A.; Mullali, G.; Schiza, D.; Sajic, M.; Hargreaves, I.; Heales, S.; Duchon, M.R.; et al. Mitochondrial dysfunction is an important cause of neurological deficits in an inflammatory model of multiple sclerosis. *Sci. Rep.* **2016**, *6*, 33249. [[CrossRef](#)]
61. Chang, J.Y.; Yu, F.; Shi, L.; Ko, M.L.; Ko, G.Y. Melatonin Affects Mitochondrial Fission/Fusion Dynamics in the Diabetic Retina. *J. Diabetes Res.* **2019**, *2019*, 8463125. [[CrossRef](#)] [[PubMed](#)]
62. Nivison, M.P.; Ericson, N.G.; Green, V.M.; Bielas, J.H.; Campbell, J.S.; Horner, P.J. Age-related accumulation of phosphorylated mitofusin 2 protein in retinal ganglion cells correlates with glaucoma progression. *Exp. Neurol.* **2017**, *296*, 49–61. [[CrossRef](#)] [[PubMed](#)]
63. Gil, A.; Martin-Montanez, E.; Valverde, N.; Lara, E.; Boraldi, F.; Claros, S.; Romero-Zerbo, S.Y.; Fernandez, O.; Pavia, J.; Garcia-Fernandez, M. Neuronal Metabolism and Neuroprotection: Neuroprotective Effect of Fingolimod on Menadione-Induced Mitochondrial Damage. *Cells* **2020**, *10*, 34. [[CrossRef](#)]
64. Gimenez-Molina, Y.; Garcia-Martinez, V.; Villanueva, J.; Davletov, B.; Gutierrez, L.M. Multiple sclerosis drug FTY-720 toxicity is mediated by the heterotypic fusion of organelles in neuroendocrine cells. *Sci. Rep.* **2019**, *9*, 18471. [[CrossRef](#)] [[PubMed](#)]
65. Vidal-Martinez, G.; Segura-Ulate, I.; Yang, B.; Diaz-Pacheco, V.; Barragan, J.A.; De-Leon Esquivel, J.; Chaparro, S.A.; Vargas-Medrano, J.; Perez, R.G. FTY720-Mitoxoy reduces synucleinopathy and neuroinflammation, restores behavior and mitochondria function, and increases GDNF expression in Multiple System Atrophy mouse models. *Exp. Neurol.* **2020**, *325*, 113120. [[CrossRef](#)]
66. Moon, M.H.; Jeong, J.K.; Lee, Y.J.; Park, S.Y. FTY720 protects neuronal cells from damage induced by human prion protein by inactivating the JNK pathway. *Int. J. Mol. Med.* **2013**, *32*, 1387–1393. [[CrossRef](#)] [[PubMed](#)]